HEFAT2008
6th International Conference on Heat Transfer, Fluid Mechanics and Thermodynamics
30 June to 2 July 2008
Pretoria, South Africa
Paper number: KD1

NUMERICAL MODELLING OF HEAT TRANSFER IN GYPSUM PLASTERBOARDS EXPOSED TO FIRE

Kontogeorgos D.A, Kolaitis D.I.* and Founti M.A.
*Author for correspondence
Laboratory of Heterogeneous Mixtures and Combustion Systems,
School of Mechanical Engineering, National Technical University of Athens,
9, Heroon Polytechniou, Polytechnioupoli Zografou, Athens 15780,
Greece,
E-mail: dkol@central.ntua.gr

ABSTRACT

A numerical code for the simulation of the one-dimensional heat transfer through a commercially available gypsum board exposed to fire is presented. A parametric study regarding the physical properties of the gypsum is carried out. The predictions obtained with the in-house developed code are in good agreement with experimental data, when temperature dependent physical properties are taken into account. The good performance of gypsum boards under fire conditions, from the fire safety point of view, due to the dehydration/calcination process and the occurring energy absorption is pointed out by the numerical results.

INTRODUCTION

Gypsum plasterboards are widely used in the building industry for a variety of applications as an aesthetically pleasing, easily worked but mechanically enduring facing material for walls and ceilings. Additionally, they are easy to apply and exhibit good mechanical and thermal properties. In the context of building fire safety, gypsum plasterboards are capable of decelerating the penetration of fire through walls and floors, due to the endothermic gypsum dehydration process that takes place in high temperature. When a gypsum board is subjected to fire, the free and chemically bound water is released and transferred through the board, absorbing energy and thus reducing the mean wall temperature. This phenomenon can be of great importance from the safety point of view, allowing sufficient building evacuation times.

A number of studies have been carried out, regarding the numerical modelling of the heat transfer effects inside a gypsum plasterboard that is exposed to fire. Mehaffey et al. [1] introduced a two-dimensional computer model in order to predict the heat transfer through gypsum-board/wood stud walls exposed to fire. Predictions were validated with four small-scale and two full-scale resistance tests showing good agreement with the experimental data.

NOMENCLATURE

δt	[s]	Time step
ε	[-]	Wall emissivity
ρ	[kg/m^3]	Density
σ	[W/m^2/K^4]	Stefan-Boltzmann constant (5.669x10^{-8})
C_p	[J/kg/K]	Specific heat
e	[-]	Convergence criterion
h	[J/kg]	enthalpy per unit mass
h_c	[W/m^2/K]	Convection coefficient
k	[W/m/K]	Thermal conductivity
$\dot{Q}'''$	[W/m^3]	Volumetric heat generation/consumption
q	[W/m^2]	Heat flux per unit area
T	[K]	Temperature
t	[s]	Time
x	[m]	Cartesian axis direction

Special characters

∂	[-]	Partial derivative operator
d	[-]	Total derivative operator
∇	[-]	Anadelta operator for space

Subscripts

0	Formation
amb	Ambient conditions
cond	Conduction
conv	Convection
i	Node
rad	Radiation
ref	Reference
tot	Total quantities expression
wall	Wall interface

Takeda and Mehaffey [2] further improved this computer model to predict heat transfer through non-insulated gypsum board wood-stud walls. Comparisons between the model

predictions and the experimental data of both small and full-scale standard fire tests showed reasonable agreement. Clancy [3] described the advances made in modelling heat transfer through wood framed walls in fire, which included a discrete method for radiative heat transfer in cavities with re-entrant corners and gaps formed by the shrinkage of wood stud cross-sections, improving temperature predictions. Thomas [4] developed a finite element heat transfer model to predict heat transfer through light timber frame wall and floor assemblies. The model was validated with a number of furnace tests including wall and floor tests, with non-standard time-temperature curves and a realistic fire. Predictions were generally adequate, but proved to be relatively inaccurate in the case of specimens subjected to temperature histories with rapid and abrupt changes.

Sultan [5] introduced a one-dimension heat transfer model for steel-stud, non-insulated, non-load bearing gypsum board wall assemblies. Manzello et al. [6] studied the performance of a gypsum wall assembly exposed to an intense real-scale compartment fire, by presenting a model including mass transfer of water vapour formed during the dehydration process. Results showed good agreement with experimental measurements for the first 1200s; beyond this point the temperature field was under predicted. In a later work, Manzello et al. [7] compared the responses of wall-size partition assemblies, composed of gypsum wallboard panels over steel studs, exposed to an intense room fire.

Axenenko and Thorpe [8] presented a finite element model of the heat transfer processes occurring in gypsum plasterboards, incorporating the concept of moving dehydration fronts from the heated to the unheated side. McGraw and Mowrer [9] investigated the flammability and the dehydration of painted gypsum wallboard. A two-step dehydration model, similar to [8], was used in order to simulate the heating and the dehydration of gypsum plasterboard. Predictions of the dehydration depth were found to be in good agreement with the experimental data. Wakili et al. [10] studied the thermal behaviour of a commercially available gypsum board under fire conditions. Experimental measurements were used to validate a numerical model based on the temperature dependence of gypsum physical properties, i.e. density, thermal conductivity and effective heat capacity. A numerical parametric study regarding the material properties of gypsum at fire temperatures was carried out in [11]. Results showed that variations of gypsum dehydration enthalpy and specific heat peak width resulted in similar temperature variations. On the other hand, variations of the peak temperature, of the specific heat and the accuracy of the thermocouple positioning had a considerable effect on the temperature evolution. The up-to-date research results highlight the need of dedicated numerical tools to account for the gypsum board property variation for a broad range of boundary conditions as well as for heat and mass transfer phenomena within the board, which is not typically accounted for in commercial software.

To account for the above, the in-house developed computer code named HEat TRansfer ANalysis (HETRAN) is presented here. The code is open source and is used here to numerically investigate the effects of variable physical properties of gypsum at elevated temperatures and the respective consequences in the fire resistance of complete plasterboards. A one dimensional transient thermal energy equation, for multi-layer building materials, is solved numerically in HETRAN, taking into account the temperature dependence of the material physical properties, as well as the time-varying boundary conditions. HETRAN is used to predict the temperature evolution inside a gypsum plasterboard sample exposed to fire. The two dehydration steps of calcium sulfate dehydrate ($CaSO_4 \cdot H_2O$) and the dissociation of calcium carbonate ($CaCO_3$) are also considered.

Thermo-chemistry of gypsum

Gypsum boards mainly consist of gypsum, which is a crystalline mineral of calcium sulphate combined with 21% by weight chemically bonded water, known as calcium sulphate dihydrate ($CaSO_4 \cdot 2H_2O$). In addition, gypsum usually contains a small amount of absorbed free water.

When gypsum is heated above 90^{o}C, the chemically bonded water dissociates from the crystal lattice and evaporates. This process, known as "dehydration" or "calcination" of gypsum, takes place between 100^{o}C and 250^{o}C and requires the absorption of a large quantity of heat. Heat transfer through the gypsum is practically delayed until the calcination process is completed.

The dissociation of the chemical bonded water takes place in two stages. In the first stage, described in Equation 1, the calcium sulphate dihydrate losses the 75% of water, resulting to calcium sulphate hemihydrate ($CaSO_4 \cdot 1/2H_2O$).

$$CaSO_4 \cdot 2H_2O + Q \leftrightarrow CaSO_4 \cdot \frac{1}{2} H_2O + \frac{3}{2} H_2O \uparrow \quad (1)$$

If the gypsum is further heated, a second reaction occurs, Equation 2, where the hemihydrate losses the remaining water to form the calcium sulphate anhydrate ($CaSO_4$).

$$CaSO_4 \cdot \frac{1}{2} H_2O + Q \leftrightarrow CaSO_4 + \frac{1}{2} H_2O \uparrow \quad (2)$$

At temperatures near 400^{o}C, a third, slightly exothermic reaction occurs, in which the molecular structure of the soluble crystal irreversibly reorganizes itself into a lower insoluble energy state (hexagonal to orthorhombic) [6,7]. This reaction is presented in Equation 3.

$$CaSO_4(\text{sol}) \rightarrow CaSO_4(\text{insol}) + Q \quad (3)$$

A reduction of gypsum mass is observed at approximately 700^{o}C, corresponding to the decomposition of $CaCO_3$, as shown in Equation 4 [10]. This step has not been properly identified by some authors [1] or has been incorrectly identified as the second dehydration step by others [5,8].

$$CaCO_3 \rightarrow CaO + CO_2 \uparrow \quad (4)$$

When the dehydration process is completed, $CaSO_4 \cdot 2H_2O$ losses two water molecules, which correspond to a weight loss of 21% in total. The decomposition of $CaCO_3$ results in the loss of one CO_2 molecule leading to a 56% weight loss of the initial amount of the calcium carbonate.

As mentioned above, during the dehydration process the chemically bonded and free water are released as water vapour. The evaporation process requires the absorption of a large quantity of heat and thus heat transmission is effectively slowed down until calcination is completed. When a gypsum board is exposed to fire, this amount of water contributes significantly to the fire resistance of the wall assembly.

THE HETRAN CODE

The energy conservation equation in a one-dimensional slab of a multiple layer material, which is solved in HETRAN, is presented in Equation 5.

$$\rho C_p \frac{\partial T}{\partial t} = \nabla \bullet (k \nabla T) + \dot{Q}''' - h \frac{\mathrm{d}\rho}{\mathrm{d}t} \frac{\partial T}{\partial t} \tag{5}$$

The enthalpy in Equation 5 is determined using the integral of the specific heat capacity, as shown in Equation 6, where h^0_{Tref} is the heat of formation at the reference temperature T_{ref}.

$$h = \int_{T_{ref}}^{T} C_p dT + h^0_{T_{ref}} \tag{6}$$

A finite volume technique [12] is used to solve the energy equation and the respective boundary conditions.

Boundary conditions

The thermal boundary conditions that can be used in HETRAN are the following:

- Adiabatic wall
- Prescribed time dependent surface temperature
- Prescribed time dependent wall heat flux
- Convection and radiation with ambient
- Conduction between two solid materials
- Convection and radiation with a fluid (as part of the computational domain)

Spatial discretization

The physical domain is divided into *N-1* cells, consisting of *N* computational nodes. The temperature is defined on the nodes and the control volumes are determined from the half – cells surrounding the nodes (Figure 1). For the internal nodes, a second order central scheme spatial discretization is used, Equation 10 [13]. The coefficients C_1 and C_2 are defined using Equation 11. In order to calculate the variables that lie in the cell faces, the harmonic mean value is used [12]. The discretized equations for the boundary conditions are similar to the Equation 10.

$$\frac{\mathrm{d}T_i}{\mathrm{d}t} = \frac{C_1 + C_2}{\left(\rho C_p\right)_{i+1/2} \frac{x_{i+1} - x_i}{2} + \left(\rho C_p\right)_{i-1/2} \frac{x_i - x_{i-1}}{2}} \tag{10}$$

$$C_1 = \left[k_{i+1/2} \frac{T_{i+1} - T_i}{x_{i+1} - x_i} - k_{i-1/2} \frac{T_i - T_{i-1}}{x_i - x_{i-1}} \right]$$
$$C_2 = \left[\dot{Q}'''_{tot,i+1/2} \frac{x_{i+1} - x_i}{2} + \dot{Q}'''_{tot,i-1/2} \frac{x_i - x_{i-1}}{2} \right] \tag{11}$$

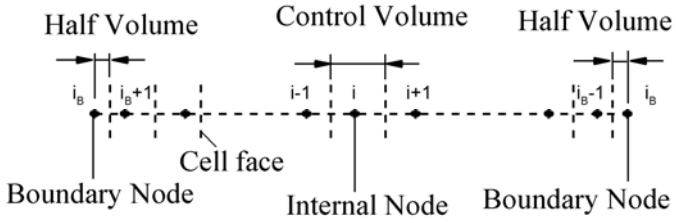

Figure 1 Control volumes

Temporal discretization

Equation 10 is cast in the general form given in Equation 12.

$$\frac{\mathrm{d}\mathbf{T}}{\mathrm{d}t} = \mathbf{F}(t, \mathbf{T}) \tag{12}$$

All calculations start with ambient conditions defined by the user (constant or space dependent). At the beginning of each time step, the temperature T^n is considered known, allowing the determination of all other quantities. In order to solve the set of equations in the form of Equation 12, a first order predictor – corrector scheme is used. The superscript $(n+1)_e$ refers to the estimation of the temperature field at the (n+1) time step. The temperature at the next time step is calculated with an explicit Euler step using Equation 13.

$$\mathbf{T}^{n+1} = \mathbf{T}^n + \delta t \mathbf{F}\left(t, \mathbf{T}^{(n+1)_e}\right) \tag{13}$$

Solution algorithm

The main steps of the solution algorithm are the following (Figure 2):

1. Initialize all temperature field and physical properties
2. For the next time step, the previous time step temperature field is set as a first estimation of the current temperature field, i.e. $T_i\,(n+1)_e = T_i\,(n)$
3. All the physical properties are calculated using the estimated temperature field
4. The new temperature field is calculated using Equation 13
5. A check is performed to confirm that the difference between the new and the estimated temperature fields for all the nodes is lower than a predefined small number, i.e. $max(T_i(n+1)-T_i(n+1)_e) \leq e$ (convergence criterion)
6. If convergence is not achieved then the new temperature field and the previous estimation is used as a new

estimation for the temperature field, i.e. $T_i(n+1)_e=\alpha T_i(n+1)+(1-\alpha)T_i(n+1)_e$, where α is the under-relaxation factor. The solution procedure goes back to step 3

7. If convergence is achieved then the procedure continues to the next time step (step 2) until the total simulation time is reached

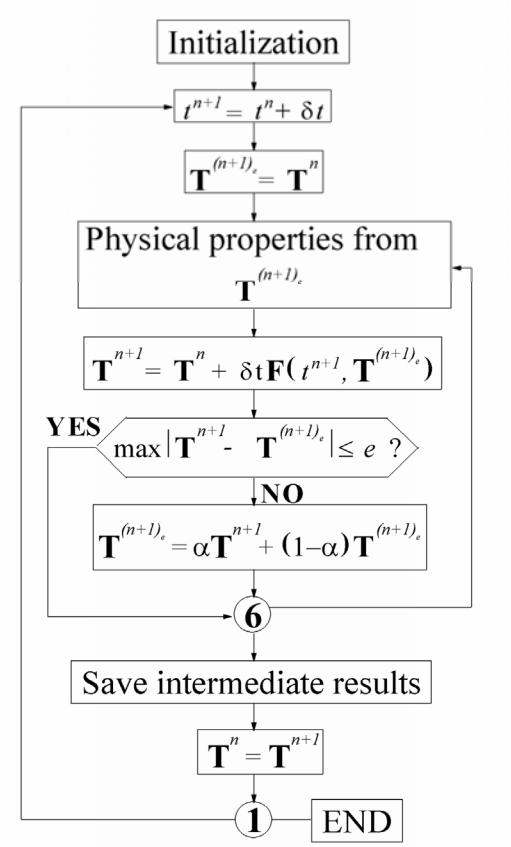

Figure 2 HETRAN solution algorithm

NUMERICAL RESULTS AND DISCUSSION

In order to validate the HETRAN code, predictions are compared with experimental data from [10]. A gypsum board plate of size 1.25m × 1.05m × 0.012m was subjected to the standard ISO 834 fire [14]. The temperature distribution within the specimen was measured by means of thermocouples placed at different depths of the samples.

The geometric model consisted of a 12mm thickness domain with a thermal boundary condition allocated to each boundary node. The "cold side" boundary condition was convection – radiation at an ambient temperature of 20°C. The form of this condition is presented in Equation 14.

$$q_{cond} = -k\left.\frac{\partial T}{\partial x}\right|_{wall} = q_{conv} + q_{rad} \quad (14)$$

The heat fluxes due to convection and radiation are determined using Equations 15 and 16, respectively.

$$q_{conv} = h_c\left(T_{amb} - T_{wall}\right) \quad (15)$$

$$q_{rad} = \varepsilon\sigma\left(T_{amb}^4 - T_{wall}^4\right) \quad (16)$$

The utilized values for the convection coefficient and the emission factor were chosen to be 10 W/m^2/K and 0.9, respectively.

For the "fire side" (x=12mm), the measured temperature [10] on the hot surface of the sample was used as a temperature boundary condition (Figure 3), thus avoiding the inaccurate procedure of defining the convective and radiative heat transfer [15].

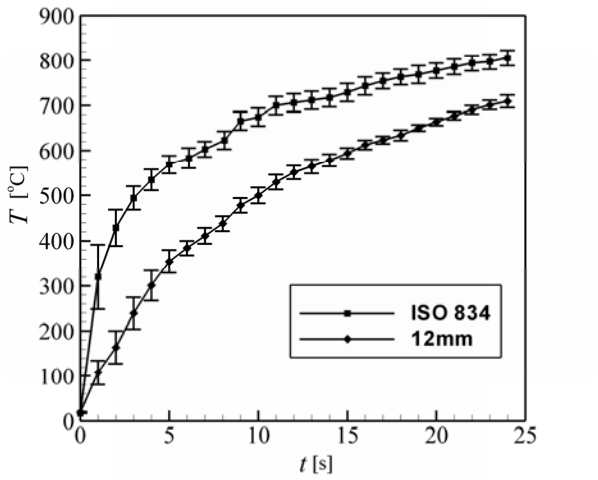

Figure 3 Furnace temperature and measured temperature on the hot surface of the sample

The physical properties for the gypsum board were obtained from the literature [10]. In Figure 4, the density of the gypsum board as a function of temperature is presented, where the two stages of weight loss are clearly shown [10].

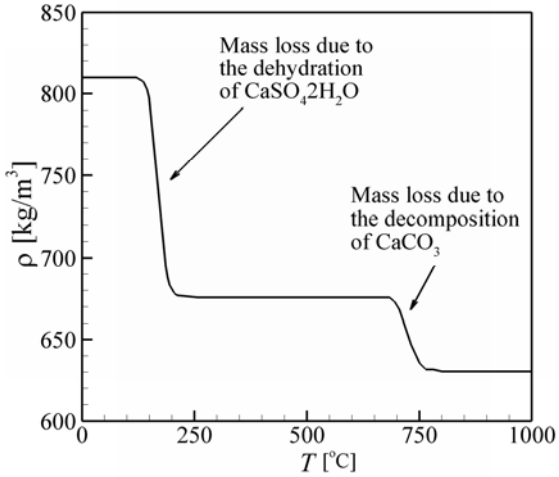

Figure 4 Density of the gypsum board as a function of temperature [10]

The specific heat of the gypsum board as a function of temperature is shown in Figure 5 [10]. The two peaks corresponding to the dehydration process lie approximately at 145°C and 200°C. The amount of endothermic energy needed for the dehydration, which corresponds to the integrated surface beneath the two peaks, is 450kJ/kg.

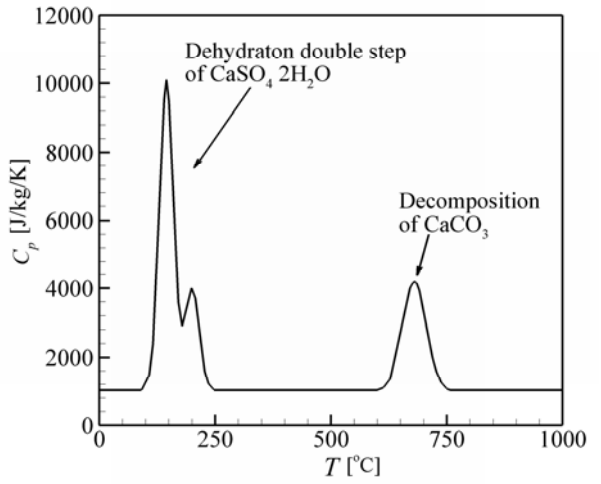

Figure 5 Specific heat of the gypsum board as a function of temperature [10]

A curve has been deduced using gypsum board thermal conductivity measurements [10] and is presented in Figure 6. The two steps of the total dehydration and the decomposition of the calcium carbonate are clearly distinguished. Initially, the sample is in its delivered condition ($CaSO_4 \cdot 2H_2O$, $CaCO_3$). After the first step the sample is fully dehydrated ($CaSO_4$, $CaCO_3$) and after the second step the calcium carbonate of the specimen is completely decomposed ($CaSO_4$, CaO).

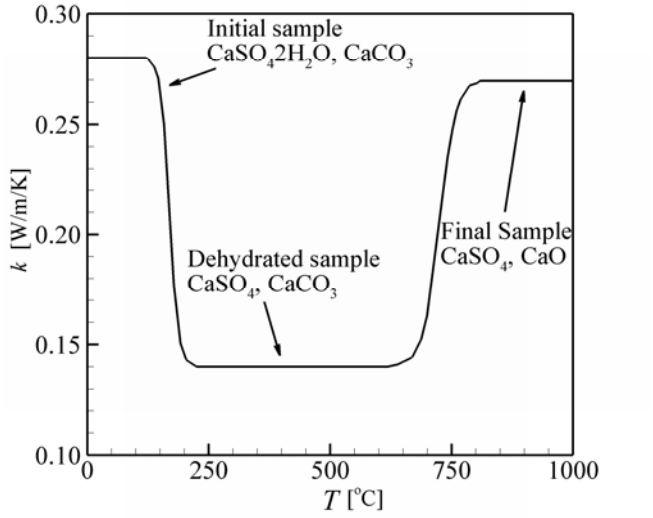

Figure 6 Thermal conductivity of the gypsum board as a function of temperature [10]

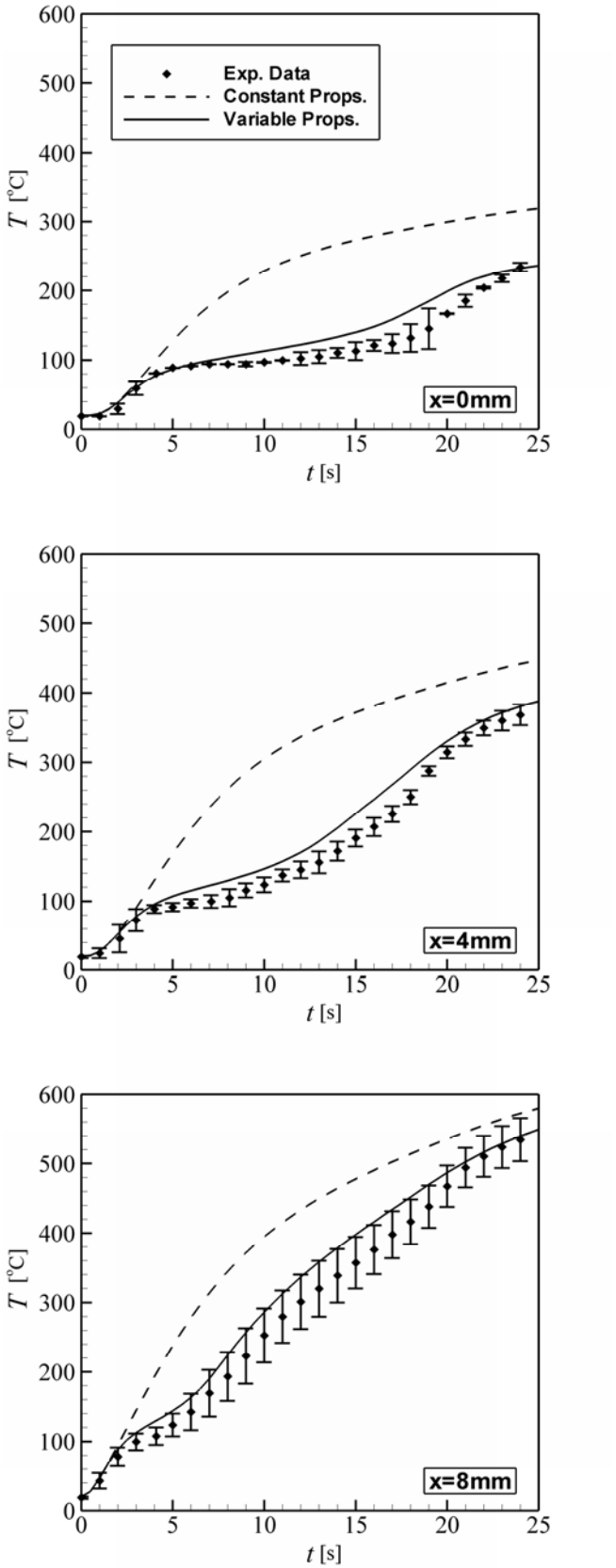

Figure 7 Comparison between calculated and measured temperature temporal evolution inside the gypsum board

Validation of the Results

In Figure 7, HETRAN predictions are compared to experiments [10] of the temperature evolution inside the gypsum board (position x=0mm corresponds to the "cold side", whereas position x=12mm corresponds to the "fire side"). In order to emphasize the influence of the temperature dependence of the physical properties, calculations performed with constant properties, i.e. ρ=810kg/m^3, C_p=1000J/kg/K and k=0.28W/m/K, as well as with temperature-dependent physical properties (Figures 4-6), are presented. It is evident that by using constant physical properties it is impossible to accurately simulate the phenomenon, because the effects of the dehydration process cannot be taken into account. On the other hand, when using the temperature-dependent physical properties, the measured temperature evolution inside the gypsum board is well reproduced by the predictions.

During the dehydration process, at temperatures between 100^{o}C and 250^{o}C, the temperature remains constant or rises at a low rate. This is more evident in the "cold side" of the gypsum board, where a temperature plateau from 5 to 13min appears (Figure 7, x=0mm). Using temperature-dependent physical properties, predictions accurately capture this behaviour, showing a very good agreement with the experimental data.

The observed small over-prediction of the calculated temperature field can be associated to the fact that with the current version of HETRAN does not account for mass transfer phenomena. Work is currently in progress to extend the code to include heat and mass transfer in porous materials. The open source nature of HETRAN gives the possibility to couple it with fire spreading simulation codes focusing on the specific behaviour of wall assemblies under fire conditions.

Finally, Figure 7 highlights the good performance of gypsum boards under fire conditions. Although the temperature in the "fire side" of the gypsum board rises significantly (Figure 3), the temperature in the "cold side" remains practically constant or rises with a low rate for a long period of time (~13min). This effect is owed to the fact that during the dehydration process the chemically bound and free water evaporates absorbing heat and thus the heat transfer through the gypsum board is retarded.

CONCLUSION

The numerical code HETRAN, developed for the simulation of one-dimensional transient heat transfer problems has been presented. The code was used for the simulation of heat transfer through a gypsum board subjected to fire conditions. The results indicated that the temperature dependence of the physical properties significantly affects the behaviour of the gypsum board. Using temperature dependent physical properties, HETRAN predictions and experimental data were found to be in good agreement. The results highlighted the need for specialized computational codes to account for the gypsum board property variation for a broad range of boundary conditions as well as for heat and mass transfer phenomena within the board. The good performance of gypsum boards under fire conditions has been demonstrated. The rate of the heat transferred through the gypsum board is slowed down, due to the endothermic reactions occurring during the dehydration process.

REFERENCES

[1] Mehaffey J.R., Cuerrier P. and Carisse G., A Model for Predicting Heat Transfer through Gypsum-Board/Wood-Stud Exposed to Fire, *Fire and Materials*, Vol. 18, 1994, pp. 297-305

[2] Takeda H. and Mehaffey J.R., WALL2D: a Model for Predicting Heat Transfer through Wood-Stud Walls Exposed to Fire, *Fire and Materials*, Vol. 22, 1998, pp. 133-140

[3] Clancy P., Advances in Modelling Heat Transfer Through Wood Framed Walls in Fire, *Fire and Materials*, Vol. 25, 2001, pp. 241-254

[4] Thomas G., Thermal Properties of Gypsum Plasterboard at High Temperatures, *Fire and Materials*, Vol. 26, 2002, pp. 37-45

[5] Sultan M.A., A Model for Predicting Heat Transfer Through Noninsulated Unloaded Steel-Stud Gypsum Board Wall Assemblies Exposed to Fire, *Fire Technology*, Vol. 32, 1996, pp. 239-259

[6] Manzello S.L., Gann R.G., Kukuck S.R., Prasad K. and Jones W., Performance of a non-load-bearing steel stud gypsum board wall assembly: Experiments and modelling, *Fire and Materials*, Vol. 31, 2007, pp. 297-310

[7] Manzello S.L., Gann R.G., Kukuck S.R. and David B.L., Influence of gypsum board type (X or C) on real fire performance of partition assemblies, *Fire and Materials*, Vol. 31, 2007, pp. 425-442

[8] Axenenko O. and Thorpe G., The modelling of dehydration and stress analysis of gypsum plasterboards exposed fire, *Computational Material Science*, Vol. 6, 1996, pp. 281-294

[9] McGraw J.R. and Mowrer F.W., Flammability and Dehydration of Painted Gypsum Wallboard Subjected to Fire Heat Fluxes, *Fire Safety Science – Proceedings of the 6th International Symposium Symposium, International Association for Fire Safety Science,* Poitiers, France, Paper number 1003, 5-9 July, 1999

[10] Wakili K.G., Hugi E., Wullschleger L. and Frank T., Gypsum Board in Fire – Modeling and Experimental Validation, *Journal of Fire Sciences*, Vol. 25, 2007, pp. 267-282

[11] Wullschleger L. and Wakili K.G., Numerical parameter study of the thermal behavior of a gypsum plaster board at fire temperatures, *Fire and Materials*, 2007, in press

[12] Patankar S.V., Numerical Heat Transfer and Fluid Flow, Hemisphere: London, 1980

[13] Trelles J. and Lattimer B.Y., Modelling thermal degradation of composite materials, *Fire and Materials*, Vol. 31, 2007, pp. 147-171

[14] International Standard ISO 834-1, Fire Resistance Tests – Elements of Building Construction – Part 1: General Requirements, 1999

[15] Wickström U., Heat Transfer by Radiation and Convection in Fire Testing, *Fire and Materials*, Vol. 28, 2004, pp. 411-415